Austenite memory and variant selection in a novel martensitic welding alloy

Conference or Workshop Item

Available online at www.sciencedirect.com

ScienceDirect

materialstoday: PROCEEDINGS

Materials Today: Proceedings 2S (2015) S325 – S331

Joint 3rd UK-China Steel Research Forum & 15th CMA-UK Conference on Materials Science and Engineering

Austenite memory and variant selection in a novel martensitic welding alloy

Steve. W. Ooi[a], Amir. A Shirzadi[b] and Jianguo Yang[c]

[a] Department of Materials Science and Metallurgy, University of Cambridge, 27 Charles Babbage Road, Cambridge CB3 0FS, UK
[b] Department of Engineering and Innovation, The Open University, Milton Keynes MK7 6AA, UK
[c] Institute of Process Equipment and Control Engineering, Zhejiang University of Technology, Hangzhou 310014, China

Abstract

The crystallographic orientation relationship between the reverse austenite and corresponding martensite in a new residual-stress-reducing weld metal was predicted, using the general theory of martensitic transformation, and verified experimentally. The theoretical and experimental results of this work also provided an evidence of the likelihood of austenite memory phenomenon.

Keywords: welding; residual stress; austenite memory.

1. Introduction

Austenite grains, which are generated from ferritic or martensitic grains, as a result of reheating cycle, tend to have identical crystallographic orientations to the original parent austenite. This phenomenon in steels is referred to as “austenite memory effect” and has been widely researched [1-8] since this effect can hinder grain refinement. During reheating process, austenite nuclei form and grow in triple points and/or along martensite boundaries before coalesce into large grains. The reverse austenite transformation can be diffusional or diffusion-less type [2, 8-10].

Most of investigations on the orientation of reverse austenite and martensite are based on the Kurdjumov–Sachs relationships [2, 4, 11]. However, it has been known that the true relation between austenite and martensite must be

doi:10.1016/j.matpr.2015.05.046

"irrational" [12-15]. Despite less than a few degrees difference in the irrational and Kurdjumov–Sachs orientations, the latter do not define the actual observed invariant–line between the parent and product lattices.

The phenomenological theory of martensite crystallography gives a complete description of the mathematical connection between the orientation relationship, the habit plane and the shape deformation for each plate that forms by the displacive transformation [12-19]. This theory has been used to design low transformation temperature (LTT) welding alloys capable of mitigating residual stresses in steel weldments, *e.g.* Camalloy 4 [20-25]. The theory is also been applied to study the transformation of austenite into a stress-induced martensite [26] or low temperature bainite [17, 27]. However, it appears that the validation of the above-mentioned theory and how variant selection occurs in a weld metal has not been performed to date. This is mainly due to the experimental limitations, which make the detection of sufficient retained austenite in low transformation temperature alloys very difficult if not impossible using laboratory equipment.

In this work, a novel low transformation temperature weld metal (Camalloy 4) was heat-treated to induce an adequate amount of reverse austenite, followed by Electron Backscatter Diffraction (EBSD) analysis to obtain the experimental data on the crystal orientations. The martensite crystallography theory [12-19] was then applied to examine the austenite memory effect as well as the effect of residual stress on variant selection during martensitic transformations in Camalloy 4.

2. Materials and sample preparation

Austenitic stainless steel (304L) base plates with the dimensions of 200 × 150 × 20 mm were used in this work. A 10 mm deep V-shape (60°) groove was machined along the centre of each plate. The sample plate was circumferentially welded onto a welding bench to obtain a fully constrained condition. The filler metal was a new alloy (CamAlloy 4), developed in the University of Cambridge, with high corrosion resistance and low transformation temperature.[28] The latter property makes this alloy capable of mitigating welding-induced residual stresses. The chemical composition of CamAlloy 4 is 0.01C, 13.0Cr, 6.0Ni, 1.5Mn, 0.7Si, 0.06Mo (wt.%). The preheating and interpass temperature were between 190-210 °C . The welding of each plate was completed in 8 separate passes, using gas metal arc welding with a shielding gas of 98%Ar-2%CO2. The welding current, voltage and speed were 230-295 A, 26-30 V and 65-78 cm per min, respectively.

For microstructural and electron backscatter diffraction (EBSD) investigation, a 10 mm thick cross-weld sample, perpendicular to the weld direction was removed from the centre of the welded plate by electro-discharge machining. The sample was then annealed at 600 °C for 1 hour to generate enough reversed austenite, before being ground and polished using conventional metallography procedures. The final polishing was carried out using colloidal silica for approximately 20 minutes.

3. Crystallographic characterisation and stress modeling

EBSD scans of all samples were performed in Camscan MX2600 SEM equipped with a field emission gun. The orientation images were taken at an operating voltage of 25 kV, a working distance of 30 mm and a tilt angle of 70°. The EBSD maps were acquired at a step size of 70 nm. Since the resolution of the mapping depends on the step size, a single pixel should not be counted as a grain.[29] Only the austenite and martensite grains with surface areas larger than the surface area of 5 pixels were analysed.

Fig. 1a shows the macrostructure of the weld together with the bead number and their positions. Point 'A' and 'B' show the approximate locations of EBSD analyses. In order to relate the EBSD data to the direction of residual stress at these points, a three-dimensional finite element (FE) analysis model was developed using *MSC.Marc* software.[30] Fig. 1b shows the mesh distribution in the FE Model consisting of 4200 solid brick elements and 5166 nodes in total.

The heat transfer coefficient was taken to be 40 W/(m^{2}K).[30] In order to model the transient heat input and effect of filler material addition, the built-in welding functionality of MSC.Marc software was used. The welding path and speed are as of the actual welding conditions. A double ellipsoid heat source with the dimensions defined in Fig. 1c was assumed.[31]

The thermal physical and mechanical properties of the base metal (304L) used in the model are reported elsewhere.[32] The yield stress of CamAlloy 4 as shown in table 1 is predicted by neural network model [33] created using available austenitic weld metal data collected from reference.[34]

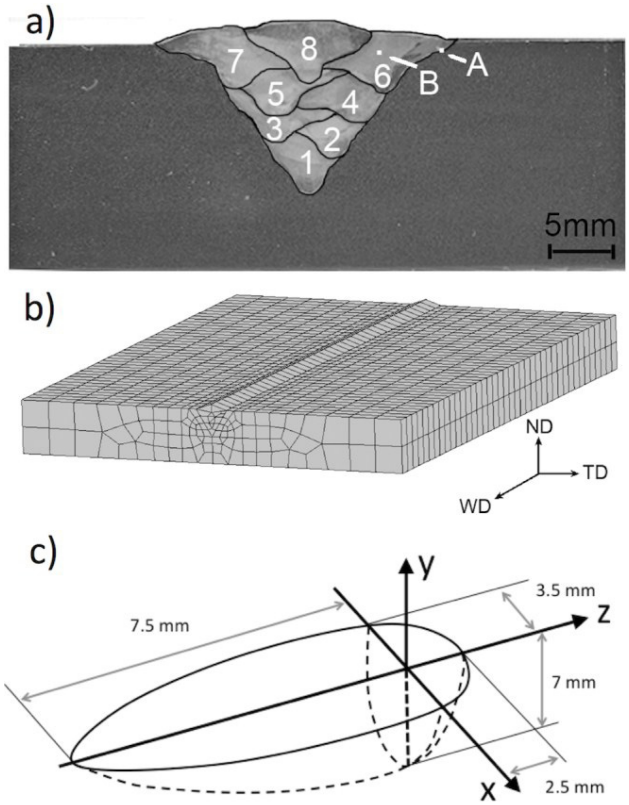

Fig. 1. (a) Weld passes and Locations 'A' and 'B' where EBSD data were obtained, (b) Mesh distribution in a 3-D finite element model and (c) dimension of assumed double ellipsoid heat source.

The simulated stress tensors corresponding to Locations A and B in Fig. 1a are as follows:

$$\begin{bmatrix} -18.3 & -8.7 & 0.5 \\ -8.7 & -10.3 & 0.2 \\ 0.5 & 0.2 & 345.5 \end{bmatrix}$$ Location A

$$\begin{bmatrix} -16.9 & -6.2 & 0.3 \\ -6.2 & -4.2 & 0.1 \\ 0.3 & 0.1 & 349.4 \end{bmatrix}$$ Location B

The stress is determined when the temperature of all weld beads reached 200 °C after the final weld pass. The axes of stress tensor are corresponded to those shown in Fig. 1b. The method used for pole figure simulation is presented elsewhere.[17, 35] The simulation of stress-induced martensitic transformation was performed using computer program *crystal_habit_poly.f* written by Kundu.[17, 35]

Table 1. Yield stress of CamAlloy 4 versus temperature as predicted by neural network [33].

Temperature / °C	Yield Stress / MPa	Uncertainty / MPa
20	425	17
100	394	18
200	363	22
300	343	29
400	332	37
500	325	46
600	316	55
700	296	63
800	260	70
900	211	73
1000	156	73

4. Results and Discussion

Fig. 2a shows the Euler images of the austenite superimposed on an EBSD image of Location A. The colour coordinated austenite grains together with the observed microstructure morphology (in the band contrast mode) were used to determine the parent austenite grain boundaries. The scanned area is in the boundary of fusion zone and base metal boundary (Location A) contains three epitaxial grains, all grown toward the centre of the weld.

Fig. 2b shows the measured and calculated 1 0 0$_\gamma$ and 1 0 0$_{\alpha'}$ pole figures of Location B. It is clear that by allowing only 12 most favoured variants, the calculated poles mirror most of the poles, which are determined experimentally. Fig. 3a shows an image in the band contrast mode of Location B in the centre of the 6th weld pass (see Fig. 1a). Very similar to Location A, by allowing 12 most favoured variants to form, the calculated poles would match most of the measured ones.

Table 2 shows the calculated interaction energy (J mol^{-1}) between a plate of martensite and the simulated applied stress based on Patel-Cohen work [16] and using the stress tensors for each of the 24 possible variants of martensite in Locations A and B. The positive values are corresponding to favourable interactions with the applied stress.

Figs. 2a and 3a are only the representative example, however, both figures show that (1) the austenite memory is present and (2) orientation relationship of austenite and martensite can be used to describe the re-formation of austenite from martensite. This indicates that the austenite nuclei can form and grow in triple points and/or along martensite lath boundaries before coalesce into large grains during inter-critical annealing. The possibility of the continuous growth from the retained austenite is however unlikely since no detectable austenite is observed in as welded condition after a carefully metallography preparation.

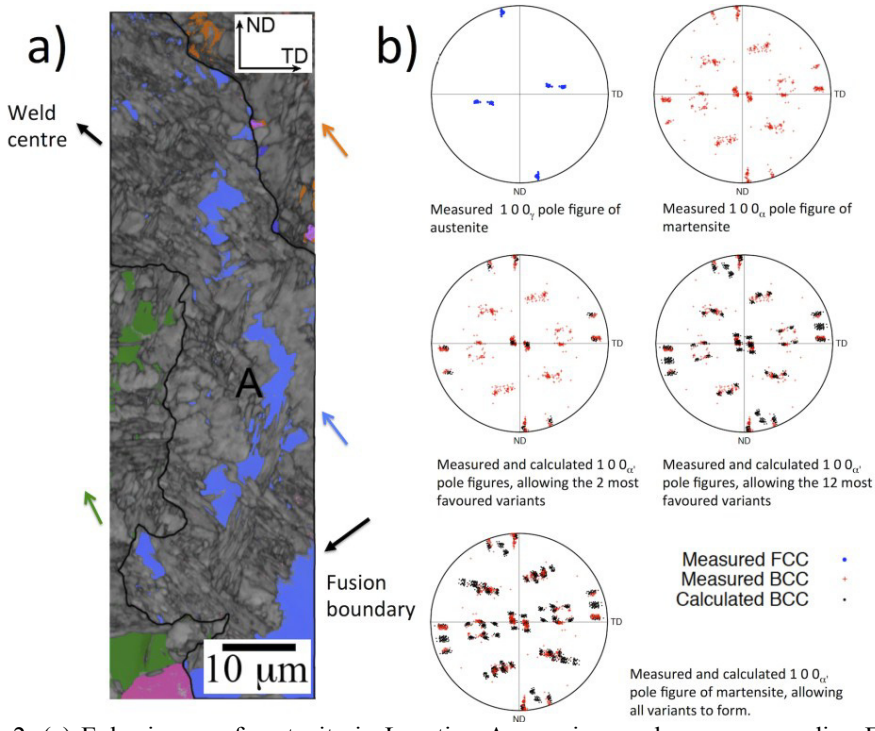

Fig. 2. (a) Euler image of austenite in Location A superimposed on corresponding EBSD image in band contrast mode and (b) Comparing the measured and calculated pole figure for Location A.

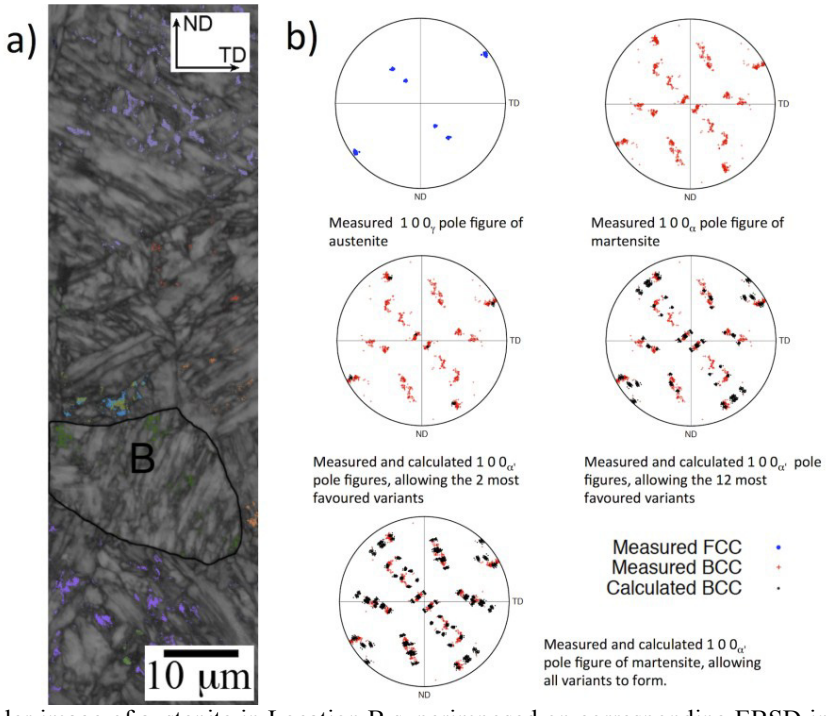

Fig. 3. (a) Euler image of austenite in Location B superimposed on corresponding EBSD image in band contrast mode and (b) Comparing the measured and calculated pole figure for Location B.

Further evidence of austenite memory is that the measured orientations of the re-formed austenite grains (in Fig. 2a) have the same orientation as the adjacent austenite grain in the base metal. It is widely known that the grain near the fusion line would grows epitaxially and has the same crystal structure to the adjacent austenite.[36] Another evidence is that the grain orientation of reverse austenite in the fusion zone is corresponding to preferential <100> crystallographic direction grown toward the centre of the weld.

Nevertheless, it is still possible that a very small amount of retained austenite, below the detection limit, has acted as a nucleation site for the re-formed austenite. This can only be verified using a more precise microstructural examination techniques, *e.g.* neutron diffraction or synchrotron diffraction for in-situ measurement.

Table 2: The interaction energy U (J mol^{-1}) between a plate of martensite and the simulated applied stress shows in the text.

Grain A		Grain B	
Variant	U	Variant	U
V8	25.9	V20	30.2
V2	25.7	V23	29.3
V10	24.3	V21	28.5
V3	22.5	V18	26.5
V21	18.1	V10	21.1
V23	17.5	V8	19.8
V22	14.7	V13	14.9
V19	12.8	V4	14.4
V24	12.6	V11	13.4
V17	10.1	V2	12.9
V20	9.5	V5	11.5
V18	8.4	V3	11.3
V6	-2.2	V15	-5.4
V11	-4.1	V24	-6.0
V13	-4.2	V12	-6.4
V16	-4.3	V22	-6.5
V14	-11.0	V9	-13.5
V15	-12.7	V1	-14.9
V7	-13.3	V6	-17.3
V9	-13.6	V14	-17.7
V4	-23.1	V19	-23.9
V5	-23.7	V17	-24.7
V12	-31.8	V16	-35.2
V1	-33.0	V7	-35.9

5. Conclusion

The main conclusions are as follows. First, the austenite memory effect is proven to be present, as the orientation relationship of the reverse austenite was consistent with those predicted by the crystallographic theory of martensite. Second, as experimentally shown, there is a strong variant selection in martensitic weld metal. However, further work is needed to investigate the possibility of the presence of a very small amount of retain austenite, which can also lead to re-formation of austenite with exactly the same crystal orientations as of the original austenite.

Acknowledgements

The authors are grateful to Ministry of Defence (MOD) for funding this work and Prof. Harry Bhadeshia for his constructive comments.

References

[1] D'Yachenko S, Met Sci Heat Treat. 42 (2000) 122-127.
[2] Kimmins ST, Gooch DJ, Met Sci. 17 (1983) 519-532.
[3] Sokolov BK, Sadovskii VD, Met Sci Heat Treat. 1 (1959) 7-14.
[4] Nakada N, Tsuchiyama T, Takaki S, Hashizume S, ISIJ Int. 47 (2007) 1527-1532.
[5] Middleton CJ, Form GW, Met Sci. 9 (1975) 521-528.
[6] Plichta MR, Aaronson HI, Metall Trans. 5 (1974) 2611-2613.
[7] Shirane T, Tsukamoto S, Tsuzaki K, Adachi Y, Hanamura T, Shimizu M, et al., Sci and Technol of Welding and Joining. 14 (2009) 698-707.
[8] Matsuda S, Okamura Y, Trans Iron Steel Inst Jap. 14 (1974) 444-449.
[9] Zhang Y, Jing XT, Lou BZ, Shen FS, Cui FZ, J Mater Sci. 34 (1999) 3291-3296.
[10] Yasuno T, Koganei A, Kuribayashi K, Hasegawa T, Horiuchi R, ISIJ Int. 36 (1996) 595-602.
[11] Song YY, Li XY, Rong LJ, Ping DH, Yin FX, Li YY, Mater Lett. 64 (2010) 1411-1414.
[12] Bowles JS, Mackenzie JK, Acta Metall. 2 (1954) 129-137.
[13] Mackenzie JK, Bowles JS, Acta Metall. 2 (1954) 138-147.
[14] Withers PJ, Bhadeshia HKDH, Mat Sci Technol. 17 (2001) 355--365.
[15] Wechsler MS, Lieberman DS, Read TA, Trans AIME. 197 (1953) 1503-1515.
[16] Patel JR, Cohen M, Acta Metall. 1 (1953) 531-538.
[17] Kundu S, Hase K, Bhadeshia HKDH, Proc R Soc London A Math. 463 (2007) 2309-2328.
[18] Christian JW, Theory of Transformations in Metal and Alloys Part 1, 3rd ed: Pergamon Press.; Oxford,2003.
[19] Christian JW, Theory of Transformations in Metal and Alloys Part 2, 3rd ed: Pergamon Press.; Oxford,2003.
[20] Ohta A, Suzuki N, Maeda Y, Hiraoka K, Nakamura T, Int J Fatigue. 21 (1999) S113-S118.
[21] Eckerlid J, Nilsson T, Karlsson L, Sci and Technol of Welding and Joining. 8 (2003) 353-359.
[22] Francis JA, Stone HJ, Kundu S, Rogge RB, Bhadeshia HKDH, Withers PJ, et al., In: Proceedings of PVP2007, ASME Pressure Vessels and Piping Division Conference, San Antonio, Texas, Year. pp. 1-8.
[23] Darcis PP, Katsumoto H, Payares-Asprino MC, Liu S, Siewert TA, Fatigue and Fracture of Eng Mater and Structures. 31 (2008) 125-136.
[24] Lixing H, Dongpo W, Wenxian W, Yufeng Z, Welding in the World. 48 (2004) 34-39.
[25] Ohta A, Matsuoka K, Nguyen NT, Maeda Y, Suzuki N, Welding Journal (Miami, Fla). 82 (2003).
[26] Kundu S, Bhadeshia HKDH, Scripta Materialia. 55 (2006) 779-781.
[27] Shirzadi AA, Abreu H, Pocock L, Klobčar D, Withers PJ, Bhadeshia HKDH, Int J Mater Research. 100 (2009) 40-45.
[28] Shirzadi AA, Bhadeshia HKDH, Karlsson L and Withers PJ, Sci and Technol of Welding and Joining. Vol. 14 (2009) No. 6 pp. 559-565.
[29] Ryde L, Mater Sci Technol. 22 (2006) 1297-1306.
[30] MSC s. MSC software.
[31] Joshi S, Hildebrand J, Aloraier AS, Rabczuk T, Comp Mater Sci. (2013).
[32] Deng D, Murakawa H, Comp Mater Sci. 37 (2006) 269-277.
[33] Bhadeshia HKDH, ISIJ Int. 39 (1999) 966-979.
[34] Voorhees HR, Freeman JW, In: ASTM special technical publication, American Society for Testing Materials, Philadelphia, Year. pp.
[35] Kundu S. Transformation Strain and Crystallographic Texture in Steels Cambridge: University of Cambridge; 2007.
[36] Kou S, Welding metallurgy, 2nd ed: John Wiley & Sons; New York,2003.